HeadSLAM - Simultaneous Localization and Mapping with Head-Mounted Inertial and Laser Range Sensors

Burcu Cinaz
TZI, Wearable Computing Laboratory
University of Bremen
Bremen, Germany
bcinaz@tzi.de

Holger Kenn
Microsoft EMIC
Aachen, Germany
holger.kenn@microsoft.com

Abstract

Self-localization of users and their wearable computers is essential to many applications, but so far, most implementation rely on a-priori information and pre-deployed infrastructures such as maps. We show how techniques from mobile robotics, namely simultaneous localization and mapping can be used to automatically generate both localization information and 2D environment maps using head-mounted inertial and laser range sensors. We present an initial implementation and the results of a number of experiments conducted in an office environment with focus on map degradation caused by shape ambiguities in the environment such as corridors.

1. Introduction

Self-localization of wearable computers and their users is one of the most important sources of context information in wearable computing and other pervasive computing applications. There are many systems in use and described in literature that use pre-deployed infrastructure for localization, ranging from global systems such as GPS to various indoor localization systems [23], e.g. based on existing or special-purpose hardware. The latter systems have in common that they use *a priori* information such as site survey data.

In situations where the environment is previously unknown, localization infrastructure can be deployed by users [13]. Systems based on inertial navigation [14, 2] can track the motions of pedestrians in buildings. However, when localization is performed in previously unknown areas, its usefulness is limited as no further information such as maps is available.

We present an approach for indoor localization and mapping that does not require *a priori* information and no user-deployed markings or beacons. This approach is especially suited for time-critical applications such as Urban Search and Rescue. In addition to the localization information, it generates a map of the environment by using techniques from mobile robotics. In mobile robotics, sensors measuring the distance to obstacles such as 2D laser-range scanners can be used to create current local maps of the environment of the robot. Matching current scans of the environment with previous scans or *a priori* map data (so-called scan matching) can be used to improve wheel-rotation odometry based position estimates of the robot and to create global maps.

The incremental acquisition of maps during exploration of previously unknown environments constitutes a fundamental problem in mobile robotics. It is referred to as the *simultaneous localization and mapping (SLAM) problem* . The complexity of this problem arises from the fact that a robot needs a map of the environment for its localization and at the same time for generating a map a robot needs to know its own position. A naive approach of creating maps by joining local maps based on odometry is possible, but with errors in map matching and odometry, global consistency of these maps degrades over time. More elaborate algorithms are used to maintain map consistency.

2. Related Work

Sensors used for SLAM are odometry and obstacle or landmark detectors. In our case we concentrate on laser scanners for obstacle detection. A so-called LADAR (Laser Detection and Ranging) measures the distance to reflecting surfaces of obstacles. Typical laser scanners perform a circular scanning measurement in a horizontal plane and return a vector of distance measurements. The vector elements correspond to individual range measurements taken at fixed angles.

There are multiple approaches to solve the SLAM prob-

lem (see [21] for a survey). The two main directions are Kalman filtering [25] and particle filtering [5, 22]. Doucet et al. [3] introduced Rao-Blackwellized particle filters (RBPF) as a solution approach for the SLAM problem. This approach applies a particle filter where each particle has its own map and represents a possible trajectory. The first implementation of this technique was FastSLAM by Montemerlo et al. [17, 18] for landmark based maps. Rao-Blackwellized particle filters were used to estimate the robot path where each individual map is represented by a set of features. In contrast to FastSLAM for landmark based maps, in the work of Eliazar et al. [4] there is no need of existing landmarks in the environment since the map is represented by evidence grids. Hähnel et al. [9, 8] extended the idea of FastSLAM with grid maps and in addition decreased the number of particles by combining scan matching with Rao-Blackwellized particle filtering. Thereby, sequences of laser measurements are used to correct the odometry measurements. This allows for a more accurate map estimation and at the same time reduces the number of particles needed for the representation of the posterior. Grisetti et al. [6, 7] extended this idea and presented an improved proposal distribution in their work GMapping which generates particles more efficiently than Hähnel's approach.

Kleiner and colleagues [12] introduced an RFID based SLAM in order to provide a better coordination between robots in search and rescue area. This approach was extended for pedestrians [10, 11]. In this technique, RFID tags are actively deployed along the path which have the information of trajectory and the explored map until that point for each pedestrian. By using this information each explored portions of the map are combined to a globally consistent map according to the method introduced by Lu and Milios [16].

In this paper, we used the GMapping implementation from Grisetti et al. [7] which is available on OpenSlam [1] as the basis for our implementation. First, we show how a Rao-Blackwellized particle filtering works in order to solve the SLAM problem and then we introduce quick solutions for the adaption of the mapping algorithm to the wearable setup.

3. Mapping with Rao-Blackwellized Particle Filters

The goal of the Rao-Blackwellized particle filters [3] is to estimate the map m and the trajectory $x_{1:t}$ of the robot given the observations $z_{1:t}$ measured and odometry controls $u_{1:t-1}$ executed so far. Since each particle possesses its own map and trajectory, it treats the entire problem as a collection of two separate sub-problems: estimation of the trajectory and the map estimation. After computing the trajectory $p(x_{1:t}|z_{1:t}, u_{1:t-1})$, the knowledge of the observation history $z_{1:t}$ is then used along with the trajectory $x_{1:t}$ to compute the map $p(m|x_{1:t}, z_{1:t})$ with the following factorization

$$p(x_{1:t}, m|z_{1:t}, u_{1:t-1}) =$$
$$\underbrace{p(m|x_{1:t}, z_{1:t})}_{\text{map estimation}} \underbrace{p(x_{1:t}|z_{1:t}, u_{1:t-1})}_{\text{trajectory estimation}}. \quad (1)$$

The main problem of the Rao-Blackwellized approach is the necessary number of particles to generate the map. Grisetti et al. [7] compute an improved proposal distribution which takes into account the most recent observations to draw the next generation of particles. Each pose of the particle is first updated according to the odometry motion model. Subsequently, a scan matching algorithm is initialized with this pose and used to correct the pose obtained from odometry data. In this manner, the particles are focused only on the important regions of the distribution. The employed scan matching technique tries to find the most likely pose by matching the current scan against a pre-built map with the following equation where $x_t^{'(i)}$ is the initial pose estimate obtained from odometry

$$\widehat{x}_t^{(i)} = \underset{x}{argmax}\, p(x|m_{t-1}^{(i)}, z_t, x_t^{'(i)}). \quad (2)$$

4. HeadSLAM - SLAM for Wearable Scenario

Grisetti et al. [7] assume the following for their implementation:

- The laser scan data comes from a heavy-duty 2D long-range laser such as a SICK LMS200[1].

- The laser scanner is mounted so that it scans a fixed horizontal plane.

- Odometry information is available from the robot platform.

In order to design a wearable system, we replaced the heavy-duty (4.5kg) long-range scanner with the much lighter (160g) short-range laser scanner Hokuyo URG[2] (cf. Figure 1).

Pedestrian motion makes it impossible to mount the scanner in a way that it scans a fixed horizontal plane. We therefore mounted an inertial measurement unit (IMU)[3] to the Hokuyo URG on the helmet in order to estimate the head motion and correct the scan data (cf. Figure 1). The IMU output consists of roll, pitch and yaw angles (φ, θ, ψ) that indicate the orientation of the sensor relative to the direction

---

[1] SICK:http://www.sick.com/
[2] Hokuyo URG:http://www.hokuyo-aut.jp/02sensor/07scanner/urg.html
[3] XSens IMU:http://www.xsens.com/

Figure 1: The test person with Hokuyo URG laser scanner and XSens IMU mounted onto her helmet.

(a) Binary classification of the walking state.

(b) Vertical peaks occurred while the person is walking.

Figure 2: Detection of the motion state as "walking" or "standing".

of gravity and the earth magnetic field. It also provides three acceleration values in the frame of reference of the sensor.

For pedestrians, there is no simple way to obtain odometry information[14, 2], i.e., consecutive motion vectors describing the motion of the pedestrian in 2D or 3D space. We implemented a simple step detection process into the motion model which detects a step occurrence of the pedestrian by observing the vertical acceleration data provided by the IMU and, together with the orientation data, gives an initial pose estimate[4].

4.1. Transformation of Scan Data

Since the head of the pedestrian is not stable while walking, the plane of measurement of the laser scanner moves and each successive set of laser scans is therefore associated with their own set of tilt angles. These scan measurements collected in 3D space cannot be used immediately as input to the SLAM algorithm without pre-processing.

First, based on the measured range of the laser scanner, we compute the 3D position of the corresponding scan point relative to the local coordinate frame of the laser scanner. Then we use the 3D affine transformation to transfer the same scan point in the global coordinate frame. Let $(x, y, 0)$ be the scan point[5], the coordinates (x', y', z') of this point in the global frame is found by multiplying it with the rotation matrix $M = R_Z(\psi)R_Y(\theta)R_X(\varphi)$
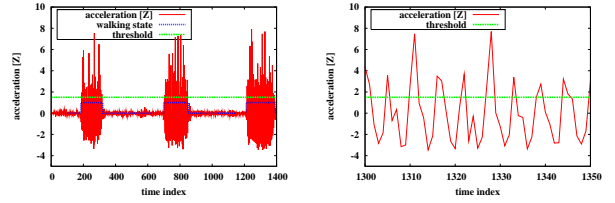
$$\begin{pmatrix} x' \\ y' \\ z' \\ 1 \end{pmatrix} = R_Z(\psi)R_Y(\theta)R_X(\varphi) \begin{pmatrix} x \\ y \\ 0 \\ 1 \end{pmatrix} \quad (3)$$

where φ, θ, ψ correspond to roll, pitch and yaw.

We project x', y', z' onto the horizontal plane and compute a new projected range d'_i for each laser beam in the

horizontal plane. This projection is correct under the assumption that walls and other objects have surfaces that are vertical. However, this assumption does not hold if the laser beam hit the ceiling or the floor. Based on a known mounting height of the sensor and assumed ceiling height, we can identify these cases and remove such beams from the data produced.

4.2. Step Detection as Initial Odometry

Our initial test was performed with the odometry information set to zero, i.e. we assumed that the scan matching implemented in the original algorithm could generate updated position information. However, the scan matching without any initial pose estimate could not give us reliable position updates to acquire a usable map. To overcome this problem, we integrated a simple motion model which detects a step occurrence by observing the vertical acceleration, similar to the approach used by Ladetto et al. [15]. If the vertical acceleration exceeds a threshold value in a defined time interval, we assume the pedestrian to be walking forward in the direction of view with a fixed speed, otherwise, we assume the pedestrian to be standing. Figure 2 shows the classification of walking state and the occurred peaks in vertical acceleration while the person is walking.

According to Ladetto et al. [15] the most natural step frequency for an average person is around 110 steps/min (~1.8Hz) and the mean step length is 75 cm. In our model, we therefore used an average linear speed of 1.35 m/sec as initial odometry guess in cases where the motion state is classified as "walking" and 0 m/sec otherwise. With the integration of step detection process, scan matching can be used to correct the position estimate.

5. Experiments

We evaluated the HeadSLAM scenario by a set of experiments. The data sets for the experiments were gathered in two distinct office environments as depicted in Figure 3. The first environment is a $40\,m$ x $17\,m$ corridor with several
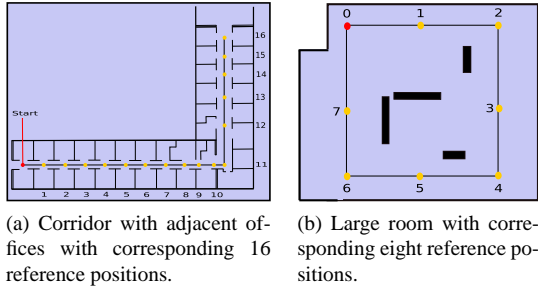
---

[4]Note that head direction and direction of motion can be different but can be measured independently at the expense of a second IMU device mounted at the hip

[5]The scanner only produces 2D data, therefore the z coordinate is set to zero

(a) Corridor with adjacent offices with corresponding 16 reference positions.

(b) Large room with corresponding eight reference positions.

Figure 3: Outline of two office environments used for experiments.

(a) Basic map output with walk trajectory.

(b) Distance error between estimated and real positions.

Figure 4: Resulting map of the corridor along with 14 open rooms and plot of localization errors.

adjacent offices(cf. Figure 3a). The second environment is a 7 x 8 m^2 room where four different obstacles were placed in the field of view at head level as shown in Figure 3b.

To provide ground-truth position information, both areas were equipped with surveyed visual markers. The corridor had 16 visual markers placed at locations along a specified path. For the experiment in the room, eight visual markers were used. The exact locations of all reference markers (i.e. in both reference scenarios) were surveyed manually using a measuring tape. When recording the data in each run, whenever a certain reference position was passed, the data from the laser scanner measured at this point in time is associated with the particular reference position by creating a time stamp.

During our experiment we configured the implementation by Grisetti to use 100 particles. A new observation was integrated to the filtering process whenever either five range scans were recorded or a rotation greater than 0.5 radians ($\sim 28°$) was observed.

5.1. Experiments with Manual Position Data

In the first experiments, we provide precise manually generated odometry input in order to obtain a performance baseline. These experiments must show the accuracy of estimated positions of predefined target markers when ideal odometry information is available. Using visual markers as reference positions, the artificial odometry data was produced by interpolating the trajectory between neighboring reference points linearly under the assumption that the translational walking speed was constant. Over the course of recording of the laser data, the view direction was kept aligned with the primary walk direction. There was no additional motion of the head other than the vertical one, which arises naturally from the lifting of the body while walking.

The first initial experiment was performed in the corridor along with 14 open office rooms. It was assumed that during the walks through the corridor the laser scanner would be able to detect portions of the adjacent offices such that
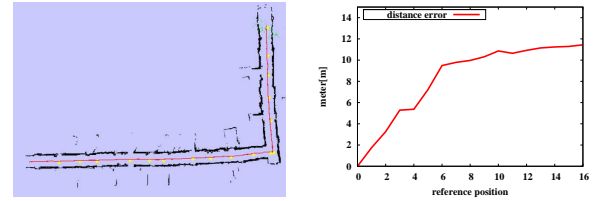
the scan matcher could correct the poses with sufficient accuracy based on the available features in the environment.

As shown in Figure 4a, the test person started at the left side of the corridor and walked with constant speed to the upper part of the corridor along an l-shaped trajectory. Each yellow point in the graphic corresponds to a visual marker placed in the corridor. Although 14 office rooms were open while taking measurements, the laser scanner was unable to detect the whole area of most of the rooms precisely. For instance due to its limited range up to four meters, it was not possible to detect the back wall of the rooms from the center of the corridor. Furthermore one side of the room was covered due to walk direction. As a consequence the existence of the rooms along the walk trajectory provided less distinctive features to facilitate scan matching than initially expected.

In order to analyze the results in a quantitative way, the distance between the estimated position and reference position was measured. Figure 4b shows the obtained error plot. It is shown that a maximum displacement error of about 12 meters occurred even though accurate position data was provided as input. When looking at the trajectory data, it can be seen that the algorithm under-estimated the real distance travelled. In cases where no object is detected in the maximum range, the scanner reports no distance information. Due to this factor, incorrect pose hypotheses are generated in the direction of the corridor.

As a working hypothesis, it was assumed that this large error value on the displacement arises due to the lack of laser-detectable features along the corridor. In order to support this hypothesis, another data set was recorded in the corridor where all office rooms were closed. In the corridor where all the rooms were closed, the error between reference and estimated position accumulates to a maximum of 18 meters. This error is much higher than in the first scenario due to the lack of accessible rooms which provide some kind of distinctive features to facilitate scan matching.

However, an error greater than 10 meters as observed in the open-door experiment limits the use of this approach in realistic application scenarios.
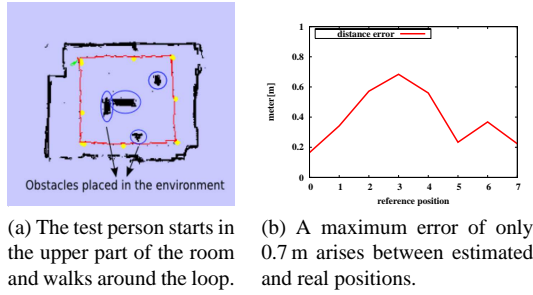
(a) The test person starts in the upper part of the room and walks around the loop.

(b) A maximum error of only 0.7 m arises between estimated and real positions.

Figure 5: Results of the data set recorded in the room with a dimension of 7 x $8\,m^2$.

Therefore, a further experiment was devised not in a corridor but in a single large room with distinct obstacles placed as depicted in Figure 5a. The room is large in respect to the maximum detectable area of the laser scanner which means that the laser scanner can still detect only one part of the room. In order to compensate for this incomplete perception and provide laser detectable objects in the range of the scanner, additional objects such as movable walls and flip charts were placed in the middle of the room. It was to investigate the influence of both the environment configuration and the existence of laser-detectable objects in the environment.

The walk trajectory of about 25m started from the zero position shown in Figure 3b and consisted of a single traversal of the reference points ending again at the starting position. Figure 5 shows the map acquired in the room and the error plot of localization errors. The maximum localization error is 0.7 meters. Good estimation of reference positions is due to existence of distinguishable obstacles in the maximum range area of the laser scanner. On the other hand, the structure of the room and the corridor looks different.

This experiments shows that there is a need for some unique obstacles in the range of laser scanner to decrease the pose uncertainty. Based on this finding, in the next experiment the same corridor is evaluated with several obstacles such as movable walls and flip charts placed along the
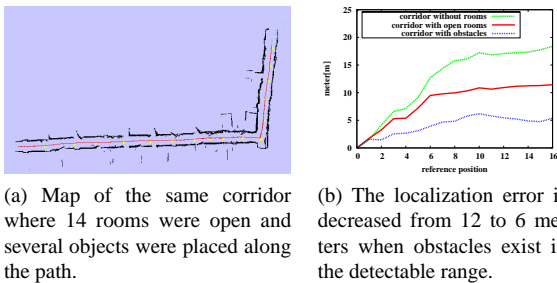

(a) Map of the same corridor where 14 rooms were open and several objects were placed along the path.

(b) The localization error is decreased from 12 to 6 meters when obstacles exist in the detectable range.

Figure 6: Results of the data set recorded in the corridor with several obstacles.

(a) Generated map of the corridor using sensor-derived position data.

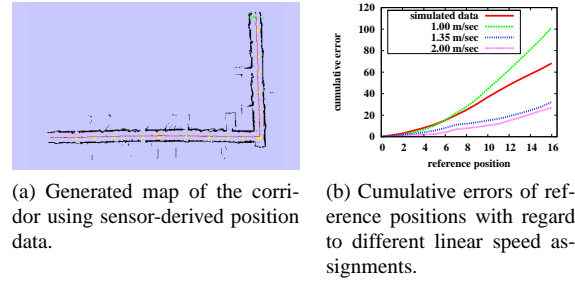(b) Cumulative errors of reference positions with regard to different linear speed assignments.

Figure 7: Results based on sensor-derived position data.

corridor such that the predefined path was not blocked. The availability of obstacles can provide that the laser scanner does not return its maximum range in the direction of corridor but distance values to those objects. Additionally, doors of the 14 office rooms were open during the data recording.

The resulting map and a comparison of position errors are shown in the Figure 6. The results show a significant decrease in the error of the pose estimation in comparison to the original corridor setup. In fact, the error rate is decreased to half the amount measured previously.

We showed that even though ideal pose information was given as input to the mapping algorithm, a large displacement error of about 12 meters develops in a featureless corridor. To show that this pose uncertainty is due to a scan matching problem, we performed another experiment in a single large room where only an error of 0.7 meters arose. The structure of the room and the existence of other obstacles in the range of laser scanner lead to a performance improvement. Thus, in the last step several movable walls and flip charts were placed in the corridor and a new data set was recorded in the same path predefined before. By doing so, the localization error could be decreased to 6 meters which amounts to only half of the original error.

5.2. Experiments with Sensor-Derived Position Data

In these experiments, we used the yaw angle data from IMU sensor for the heading direction. Moreover, we created odometry data from our simple motion model based on step detection. The model assumes a default fixed translational velocity of 1.35 m/sec in cases where the motion state is classified as "*walking*" and 0 m/sec otherwise. We compared localization and mapping results using manually generated poses and odometry poses obtained from sensor data. Figure 7a shows the resulting map with default translational velocity of 1.35 m/sec. Different cumulative errors for each of speed values are shown in Figure 7b.

As can be seen from the figure, the cumulative errors decrease inversely proportional to linear speed values. Apparently, the error rate reaches its minimum if the average lin-

(a) Map generated with a given linear speed of 1.35 m/sec.

(b) Map generated with a given linear speed of 2.00 m/sec.

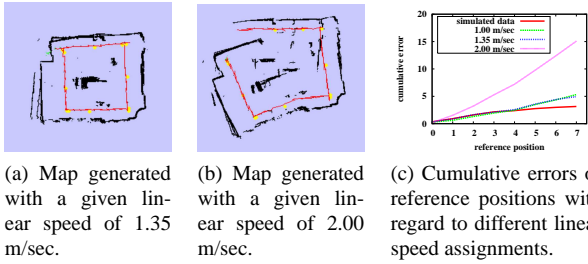(c) Cumulative errors of reference positions with regard to different linear speed assignments.

Figure 8: Mapping results and cumulative error plot of the data set recorded in the large room.

ear speed per second for walking was taken as 2.00 m/sec. However, this speed value exceeds the average linear speed of ~ 1.2 m/sec of the pedestrian which was measured during recording. A high speed value of 2.00 m/sec eliminates the general scan matching problem which drags the position of the pedestrian back because of very similar structure of the corridor. However, it does not mean that a higher value is optimal under other circumstances. An extreme estimation for the translational velocity can lead to severe inconsistencies in the environment map as shown in Figure 8. The evolution of errors was inverse there as the error became larger proportional to linear speed values such that 2.00 m/sec gave the largest error. Figure 8 shows that the localization error was minimal when manually generated precise odometry was used. Furthermore, the default value of 1.35 m/sec for the average linear speed gave by far the closest result to this simulation, contrary to the corridor case.

In another experiment, we carried out a large amount of head motion during data recording in the corridor (i.e. corridor with several obstacles along the path). Figure 9 shows the acquired map and the trajectory. The map includes measurements affected by a high level additional of head motion along all three degrees of freedom. The difference of the trajectory which is caused by the additional head motion is quite obvious to detect in the figure. The path follows a
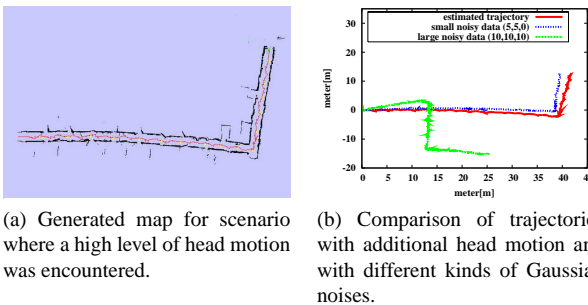

(a) Generated map for scenario where a high level of head motion was encountered.

(b) Comparison of trajectories with additional head motion and with different kinds of Gaussian noises.

Figure 9: Influence of the head motion on the map and the noise behavior of this effect.
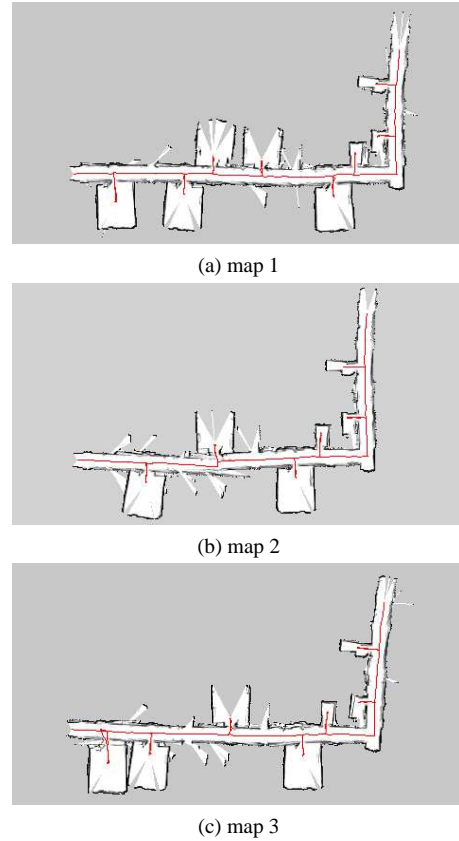

(a) map 1

(b) map 2

(c) map 3

Figure 10: Maps of three different run throughout the corridor where different number of rooms are explored.

zigzag course because of the difference between the human body motion and a typical car-like robot motion. The human body can move holonomically along the path, which means that it can move in any direction while at the same time controlling the rotation of the head. However, non-holonomic car-like robots are restricted to move always in the direction of the its heading orientation. The typical motion models used for map and localization estimate are those which are restricted by non-holonomic constraints.

In order to analyze position errors that occur due to the head motion in different directions while walking straight, different kinds of Gaussian noise were added to the odometry information of the data recorded without head motion. When looking resulting maps for each noise set, we saw that the motion of the head causes some noise in $\langle x, y \rangle$ locations because of its holonomic behavior. This comparison can be seen in Figure 9b. The trajectory estimated with head motion was closest to the one obtained with a noise of $\langle 5, 5, 0 \rangle$[6]. The other trajectory in the figure shows that a noise added to the heading direction effects the estimated

---

[6]The values $\langle x, y, \theta \rangle$ correspond to the standard deviation of the Gaussian noise with the units: centimeter, centimeter, degree
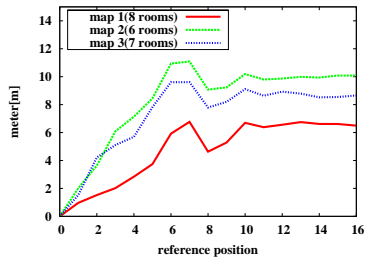
Figure 11: Localization errors occurred in each data set.

Figure 12: Occupancy grid map of the corridor when the same path traversed back and a loop closure is performed.

positions drastically.

5.3. A More Complex Structure

This experiment was carried out in the same corridor presented above where additional rooms were entered during data acquisition (cf. Figure 3a). Three different data sets were recorded in which a different number of rooms are explored. Besides, while exploring the inside of the rooms, the walk action was stopped repeatedly for short periods of time. We used sensor-derived position data for these experiments.

Figure 10 shows the generated occupancy grid maps for each data set. Moreover, the localization errors of the reference positions are investigated once again. As before, the distances between real and estimated positions of the reference points are measured. Figure 11 shows error plots for each map. According to these results, the localization error decreases inversely proportional to number of visited rooms. This is due to the laser scanner gaining more information while exploring in contrast to the situation in a featureless corridor. The more rooms are explored during data gathering, the better are the localization results. The error is minimal with a value of six meters in Figure 10a where eight rooms are visited along the corridor. In Figure 10b, the localization error is a a maximum with 10 meters. Here, only a minimum number of six rooms were visited.

A particularly difficult problem in map acquisition is loop closure. Whenever a large cycle is traversed in the environment, it must be recognized that currently perceived sensor data matches previously compiled parts of the map which leads to hard data association problems. In order to analyze the ability of HeadSLAM to perform loop closure, we employed the same data sets used above along with their second part where the same rooms were visited in reverse order on the way back to the original starting point[7]. Figure 12 shows one of the three maps (Figure 10a) where a

---

[7]Since large structures with several loops were not available in the environment where the experiments of HeadSLAM were performed, the tests were constrained to the same corridor where predefined path and same rooms were revisited on the way back.
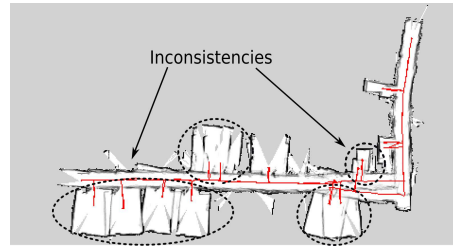
loop closure was performed. As can be seen from the figure, even though the first two rooms on the right side of the corridor can be associated truthfully on the way back, the rooms which were visited first cannot be recognized correctly and thus alignment errors occur as depicted in the figure. One of the main reasons why the application was unable to close the outer loop correctly was that the particles which were required later to close the loop correctly were deleted too early which is also known as particle deprivation problem [24]. Whereas in the context of mobile robotics, methods exist [20] to reduce this risk by forcing the robot to leave an inner loop and to explore unknown areas, these techniques are generally not directly applicable in the considered wearable scenarios due to the idiosyncrasies of the scenario rather than for technical reasons.

6. Conclusion and Future Work

In this paper, we presented how simultaneous localization and mapping can be used by pedestrians to acquire maps of previously unknown environments. We presented modifications for the wearable setup such as the processing for unstable head motion and the creation of odometry information. We tested our approach in a number of experiments.

We showed that the existence of distinguishable obstacles in the range of the laser scanner improves the performance of scan matching and consequently the estimation of poses. When different laser detectable obstacles were made available in a corridor, the localization error could be cut in half (from 12 to 6 meters). Moreover, we investigated the effects of different linear walking speeds on the quality of map compilation and localization. We analyzed the noise behavior of the head motion and its effects on the estimated trajectory as well as on the map. We found that the holonomic motion of the human body leads to appearance of noises on the estimated locations. We recorded different data sets in a more complex structure and we evaluated the ability of our approach to perform loop closures. We showed that the more areas explored, the better is the performance of the scan matching and thus the localization re-

sults.

In order to overcome encountered problems of scan matching with a short-range laser scanner in featureless structures, a modified version of scan matching described in [19] will be used and evaluated in future experiments. Furthermore, improved pedestrian localization systems will be integrated in order to provide a better initial pose estimate. Equipping the pedestrian with a visual camera can also be an alternative to obtain a better pose information by using 3D visual odometry. Combining our approach with RFID based SLAM may overcome the problems encountered during loop closures. A further step will be the application of this scenario to acquire 3D maps of the environment.

References

[1] Gmapping. http://www.openslam.org/gmapping.html.

[2] S. Beauregard, M. Klepal, and Widyawan. Indoor PDR performance enhancement using minimal map information and particle filters. In *ION/IEEE Position, Location and Navigation Symposium (PLANS '08)*, 2008.

[3] A. Doucet, N. de Freitas, K. Murphy, and S. Russel. Rao-Blackwellized particle filtering for dynamic Bayesian networks. In *Proceedings of the Sixteenth Conference on Uncertainty in Artifical Intelligence (UAI)*, pages 176–183, Standford, 2000.

[4] A. Eliazar and R. Parr. DP-SLAM:fast, robust simultaneous localization and mapping without predetermined landmarks. In *Proceedings of International Joint Conference on Artifical Intelligence*, pages 1135–1142, 2003.

[5] D. Fox, S. Thrun, and W. Burgard. *Particle Filters for Mobile Robot Localization*, chapter Sequential Monte Carlo Methods in Practice, pages 499–516. 2001.

[6] G. Grisetti, C. Stachniss, and W. Burgard. Improving grid-based slam with rao-blackwellized particle filters by adaptive proposals and selective resampling. In *Proceedings of the IEEE International Conference on Robotics and Automation (ICRA)*, pages 2443–2448, Spain, 2005.

[7] G. Grisetti, C. Stachniss, and W. Burgard. Improved techniques for grid mapping with rao-blackwellized particle filters. *IEEE Transactions on Robotics*, 32:16–25, 2006.

[8] D. Hähnel. *Mapping with Mobile Robots*. PhD thesis, Albert-Ludwigs-Universität Freiburg, 2004.

[9] D. Hähnel, W. Burgard, D. Fox, and S. Thrun. An efficient FastSLAM algorithm for generating maps of large-scale cyclic environments from raw laser range measurements. In *Proceedings of the Conference on Intelligent Robots and Systems (IROS)*, pages 206–211, Las Vegas, NV, USA, 2003.

[10] H. Kenn, N. Behrens, and A. Kleiner. Optimizing indoor PDR performance with self-deployed position markers. In *IFAWC 4th international forum on applied wearable computing*, pages 107–114, 2007.

[11] A. Kleiner, C. Dornhege, and S. Dali. Mapping disaster areas jointly: RFID-coordinated SLAM by humans and robots. In *Proceedings of the IEEE International Workshop on Safety, Security and Rescue Robotics (SSRR)*, pages 1–6, Rom, Italy, 2007.

[12] A. Kleiner, J. Prediger, and B. Nebel. RFID technology-based exploration and SLAM for search and rescue. In *Proceedings of the IEEE/RSJ International Conference on Intelligent Robots and Systems (IROS)*, pages 4054–4059, Beijing, China, 2006.

[13] A. Kleiner and D. Sun. Decentralized SLAM for pedestrians without direct communication. In *Proceedings of the IEEE/RSJ International Conference on Intelligent Robots and Systems (IROS 2007)*, pages 1461–1466, San Diego, California, 2007.

[14] Q. Ladetto, V. Gabaglio, B. Merminod, P. Terrier, and Y. Schutz. Human walking analysis assisted by dgps. In *Proceedings of the Symposium on Global Navigation Satellite System (GNSS)*, 2000.

[15] Q. Ladetto, V. Gabaglio, B. Merminod, P. Terrier, and Y. Schutz. Human walking analysis assisted by DGPS. *Global Navigation Satellite System, GNSS,Edinburgh, Scotland*, 2000.

[16] F. Lu and E. Millios. Globally consistent range scan alignment for environment mapping. *Autonomous Robots*, 4(4):333–349, 1997.

[17] M. Montemerlo, S. Thrun, D. Koller, and B. Wegbreit. Fast-SLAM: A factored solution to the simultaneous localization and mapping problem. In *Proceedings of the AAAI National Conference on Artifical Intelligence*, pages 593–598, Edmonton, Canada, 2002.

[18] M. Montemerlo, S. Thrun, D. Koller, and B. Wegbreit. Fast-SLAM 2.0: An improved particle filtering algorithm for simultaneous localization and mapping that provably converges. In *Proceedings of the Sixteenth International Joint Conference on Artifical Intelligence (IJCAI)*, 2003.

[19] C. Stachniss, M. Bennewitz, G. Grisetti, S. Behnke, and W. Burgard. How to learn accurate grid maps with a humanoid. In *Proceedings of the IEEE International Conference on Robotics and Automation (ICRA)*, Pasadena, CA, USA, 2008.

[20] C. Stachniss, G. Grisetti, and W. Burgard. Recovering particle diversity in a Rao-Blackwellized particle filter for SLAM after actively closing loops. In *Proceedings of the IEEE International Conference on Robotics and Automation (ICRA)*, 2005.

[21] S. Thrun. *Exploring Artificial Intelligence in the New Millennium*, chapter Robotic Mapping: A Survey. Morgan Kaufmann, 2002.

[22] S. Thrun. Particle filters in robotics. In *Proceedings of the 17th Annual Conference on Uncertainty in AI (UAI)*, 2002.

[23] P. Tome, R. Challamel, D. Harmer, and S. Beauregard. Performance assessment of indoor location technologies. In *ION/IEEE Position, Location and Navigation Symposium (PLANS '08)*, 2008.

[24] R. van der Merwe, N. de Freitas, A. Doucet, and E. Wan. The Unscented Particle Filter. In *Advances in Neural Information Processing Systems 13*, December 2000.

[25] G. Welch and G. Bishop. An introduction to the Kalman filter. Technical report, University of North Carolina at Chapel Hill, Chapel Hill, NC 27599-3175, 1995.